SOPHION BIOSCIENCE

charles river

Application Report

VHalf adaptive protocols on Qube

New online adaptive protocol for VHalf measurements on the Qube high throughput automated patch clamp platform improves control of voltage-gated ion channel state leading to reduced data variability and better-quality compound testing results

Introduction

Voltage-gated sodium (Na_V) channels have been studied extensively due to their potential as targets for several indications, such as pain, epilepsy, cardiac and muscle paralysis syndromes (Catterall et al., 2005; Catterall and Swanson, 2015; Ahern et al., 2015; Bennett et al., 2019). These channels are known to be modulated by several compounds, which are state-dependent, and bind preferentially to the inactivated state of the channel. In recent years, significant efforts have been made in elucidating the structure of Na_V channels (Lenaeus et al., 2017; Sula et al., 2017), and several novel and highly selective compounds have been shown to bind to the voltage-sensor domain 4 of the S4 transmembrane segment of $Na_V1.7$ (Ahuja et al., 2018; Alexandrou et al., 2016). The potency of these compounds is also known to vary depending on the % inactivation of the channels (Theile et al., 2016).

Na_V channels typically have steep slopes in the Boltzmann fits used to determine the VHalf of inactivation, as shown in Figure 1 for $Na_V1.1$. As a consequence, very small changes in the voltage applied to the cells may lead to the channels being more or less inactivated than the desired value.

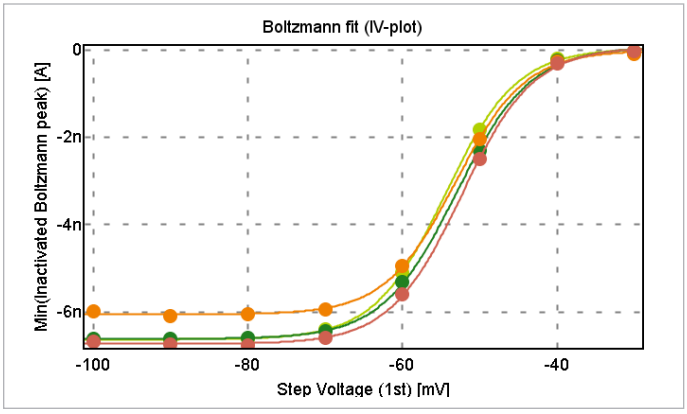

Fig. 1: Boltzmann fits for $Na_V1.1$ from four separate cells, demonstrating the typical steep slopes characteristic of voltage-gated sodium channels.

When experimenting on voltage-gated ion channels, it is imperative that the voltage applied to the cells is accurate. This is especially important, when testing state-dependent compounds. For the most accurate compound activity determinations, ideally the precise value for the VHalf of inactivation should be used for each cell. This method has been previously used in manual patch clamp and PatchXpress automated patch clamp experiments. However, it has not been possible to utilise this method on higher throughput automated patch clamp platforms, where the greatest benefit could be achieved for testing potentially several thousand compounds per day in screening campaigns, or in later stage compound potency generation where high quality and accuracy is required. Instead, the average VHalf of inactivation has been determined for a population of cells, and this value was applied to all of the cells. Due to the cell-to-cell variability in the actual VHalf of inactivation, this meant that the channels were not inactivated to the same level.

Recently, Sophion released the adaptive protocol block for the Qube 384-well automated patch clamp platform. Using this new protocol, it is possible to separately define the voltage applied to each individual well for both the activation and inactivation of the channels, enabling the generation of more precise data for voltage-gated ion channels.

Results and discussion

The VHalf of inactivation values derived from the online Boltzmann fit for the standard and adaptive experiments were very similar, as shown below in Figure 2. Therefore it could be concluded that any variability in the results between the experiments should not be due to a significant difference between the VHalf of inactivation values.

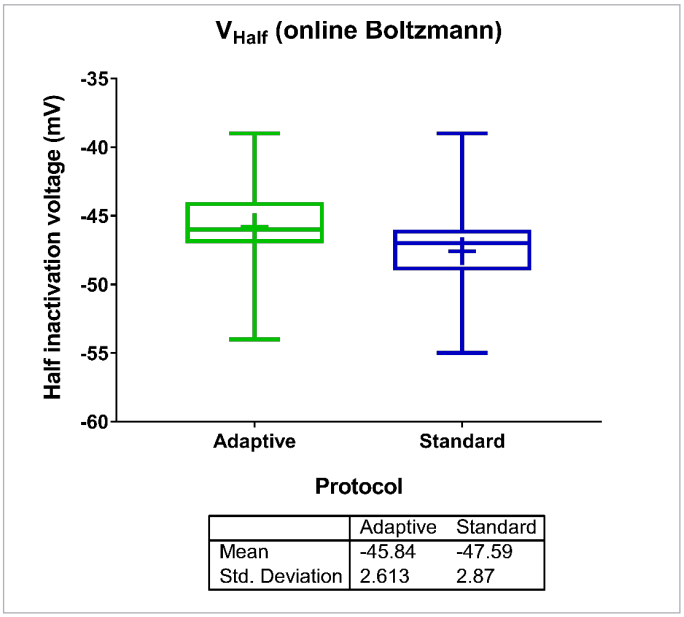

	Adaptive	Standard
Mean	-45.84	-47.59
Std. Deviation	2.613	2.87

Fig. 2: VHalf of inactivation values derived from the online Boltzmann experiment block for the experiments using either the standard voltage protocol, or the adaptive voltage protocol. As shown in the graph, the values are very similar between the two experiments. The mean values are indicated by the '+' symbol, median values by the line in the box.

The adaptive protocol did not change the performance of the assay compared to the standard protocol, as summarised below in Table 1. The seal resistance, series resistance and capacitance values remained stable before and after the online Boltzmann fit block in the experimental protocol. Both experiments had similar success rates, at approximately 75%.

Table 1: Assay performance parameters before and after the online Boltzmann fit in the experimental protocol. No differences were observed in the parameters.

	Success rate	Seal resistance (GΩ)		Series resistance (MΩ)		Cell capacitance (pF)	
		Before	After	Before	After	Before	After
Standard	73%	2.4 ±1.2	3.1±1.9	7.4±2.2	8.6±2.5	16.4±6.2	16.4±6.2
Adaptive	76%	2.1±1.9	2.5±2.0	7.4±2.7	8.1±2.5	16.7±5.5	16.3±5.5

As expected, using the individual VHalf of inactivation values in the adaptive protocol, derived for each well from the online Boltzmann fit, significantly decreased the variability of the % current inactivation, calculated as a ratio from the resting state current amplitude to the inactivated state current amplitude. These results are shown below in Figure 3, demonstrating how the use of the adaptive protocol ensures the channels in each well are inactivated to the desired level.

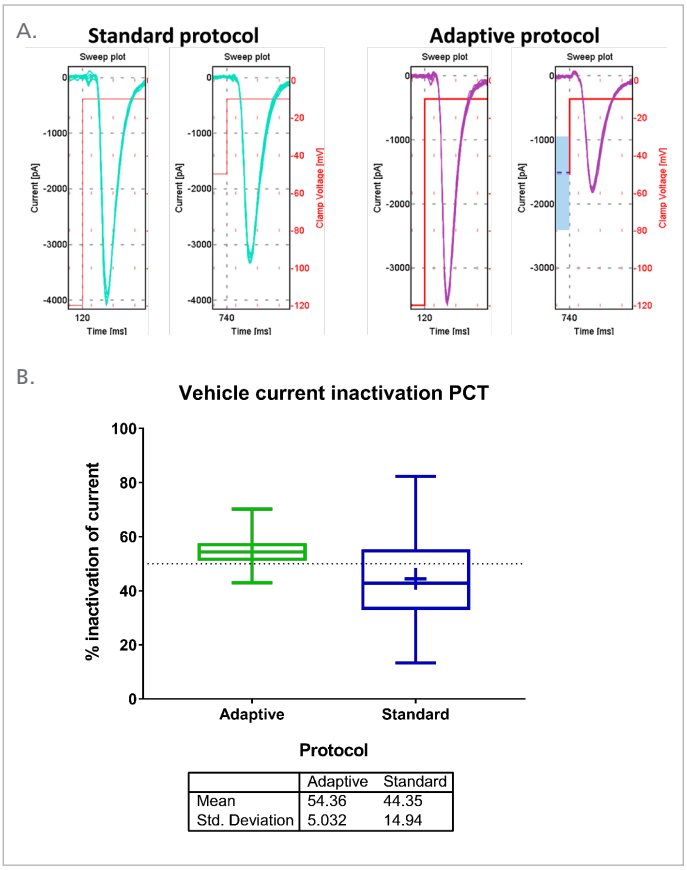

	Adaptive	Standard
Mean	54.36	44.35
Std. Deviation	5.032	14.94

Fig. 3: A) Example $Na_V1.1$ current traces from the resting state and inactivated state for the standard protocol, where a fixed inactivation voltage of -50 mV was applied, and the adaptive protocol, where the VHalf inactivation voltage was determined by the online Boltzmann fit. B) Bar graph of % inactivation of the $Na_V1.1$ current in the pre-compound vehicle period, calculated as a ratio of the inactivated state current amplitude to the resting state current amplitude. The mean values are indicated by the '+' symbol, median values by the line in the box. The variability in the % inactivation of the current is significantly reduced, when using the adaptive protocol.

In the standard protocol experiment approximately 80% of the wells had % inactivation of the current between 26 and 66. In the adaptive protocol experiment, the % inactivation of the current was between 47 and 61 for 80% of the wells. These results are summarised in the histogram below in Figure 4, highlighting how much the variability was reduced, when using the individual VHalf of inactivation values for each well.

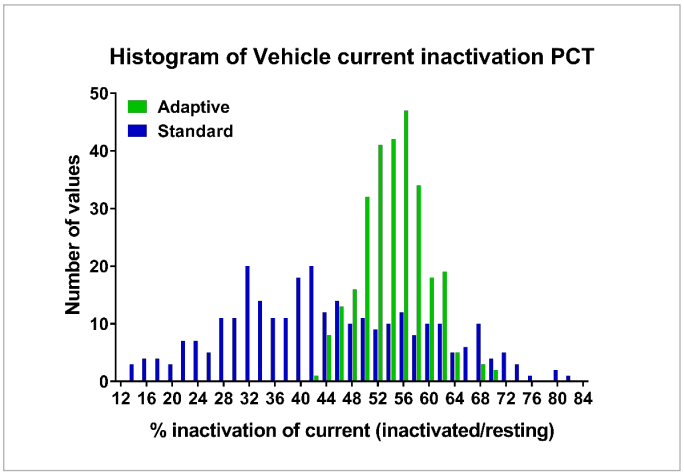

Fig. 4: Histogram of the % inactivation of the $Na_V1.1$ current, calculated as a ratio of the inactivated state current amplitude to the resting state current amplitude. In the standard protocol experiment approximately 80% of the wells had % inactivation of the current between 26 and 66. In the adaptive protocol experiment, the % inactivation of the current was between 47 and 61 for 80% of the wells.

As a consequence of the increased control in % inactivation of the current, the % inhibition results of the $Na_V1.1$ current by state-dependent compounds should also be less variable, as the channels in all wells are inactivated to the same level. Four compounds, amitriptyline, tetracaine, lidocaine and mexiletine, were tested as concentration-response curves. Examples for tetracaine and amitriptyline are shown below (Figure 5). Compound potencies were found to be similar between the protocols.

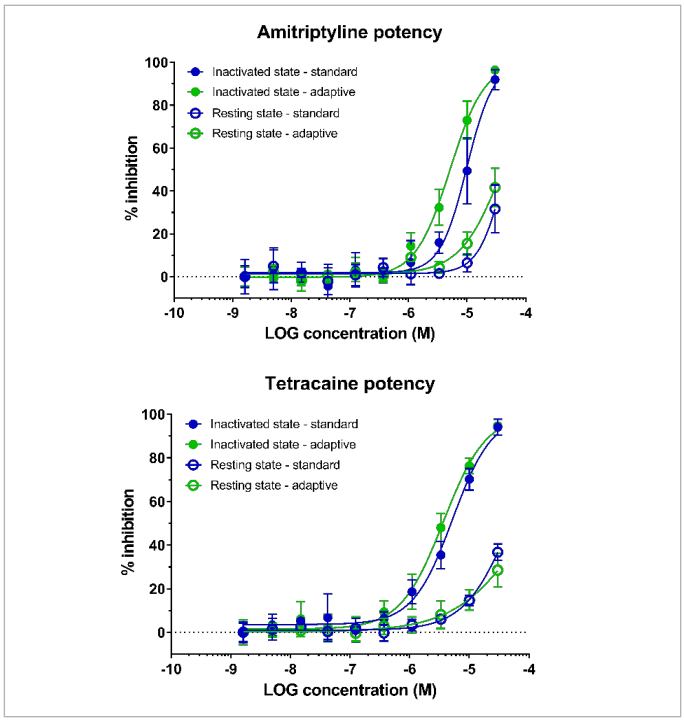

Fig. 5: Example concentration-response curves for amitriptyline and tetracaine from the resting state and inactivated state pulse of the protocol, using either the standard or adaptive experiment protocol.

When examining the compound data at 10 µM, as expected, the % inhibition data with these compounds was less variable in the adaptive protocol experiment, as shown in Figure 6 below. In the context of high throughput screening, this reduced variability should lead to increased confidence in the results, when compound % inhibition data becomes more reliable. As shown in Figure 6, the compound data in the standard protocol experiment was so variable, that in some cases the wells might not have been detected as 'hits' – for instance, if the hit limit had been set to 50% inhibition, some of the 10 µM amitriptyline wells would have been missed. Similarly, if the hit limit had been set to 30% inhibition, most of the 10 µM lidocaine wells would have been missed.

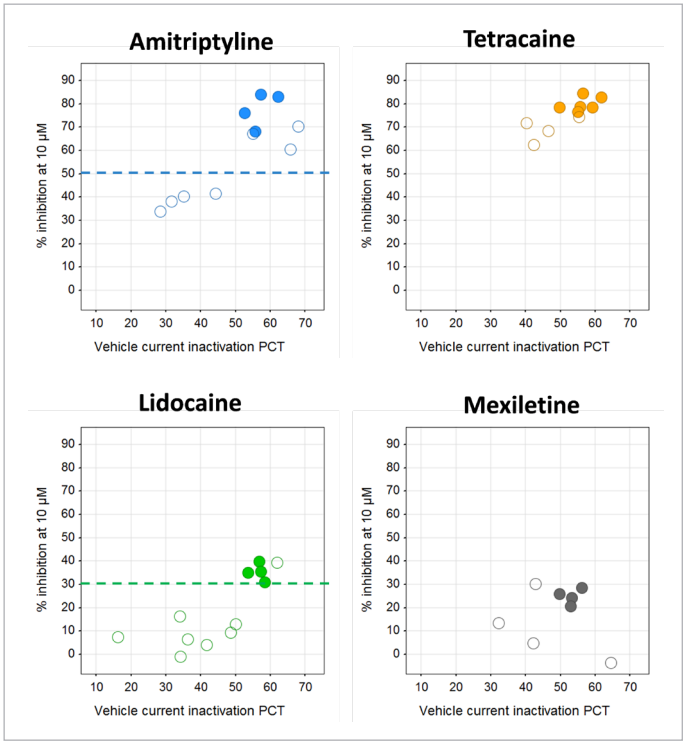

Fig. 6: Compound % inhibition data for 10 µM amitriptyline, tetracaine, lidocaine and mexiletine using either the standard experiment protocol (empty circles) or adaptive experiment protocol (full circles). As shown in the graph, the % inhibition data for all compounds was less variable using the adaptive experiment protocol. If the hit limit had been set to 50% inhibition (blue dashed line), some of the 10 µM amitriptyline wells would have been missed. Similarly, if the hit limit had been set to 30% inhibition (green dashed line), most of the 10 µM lidocaine wells would have been missed.

Conclusion

In summary, the new adaptive protocol enables increased control of the state that voltage-gated channels are in during an experiment, leading to reduced variability of data and increased confidence in compound testing results, on a 384-well high throughput automated patch clamp platform.

Methods

At Charles River, this new protocol was beta-tested using HEK $Na_V1.1$ cells. Single-hole QChip 384-well consumables were used in the experiment, whereby $Na_V1.1$ currents were recorded from a single cell in each well. The external buffer solution contained (in mM): 145 NaCl, 4 KCl, 10 HEPES, 10 glucose, 1 MgCl2, 2 CaCl2, pH 7.4 (NaOH). The internal buffer solution contained (in mM): 120 CsF, 20 CsCl, 10 NaCl, 10 HEPES, 10 EGTA, pH 7.3 (CsOH). Experiments were conducted using Sophion Qube software version 2.4.64 (Eagle). The experimental protocol was adapted from a previously used HTS screening protocol, which contained a voltage protocol aimed to inactivate the channels by 50%, using a pre-determined inactivation voltage of -50 mV for 500 milliseconds. The modified protocol is shown below in Figure 7. Series resistance compensation was applied at 70%. Currents were sampled at 25 kHz, with cutoff at 5 kHz and Bessel filtering.

The online Boltzmann fit was added into the protocol before the pre-compound vehicle period, and used to calculate the VHalf of inactivation for each well. In the standard experiment, the inactivation voltage was kept at -50 mV, whereas in the adaptive experiment the VHalf of inactivation value from the online Boltzmann fit was applied to the pre-compound vehicle and compound application periods.

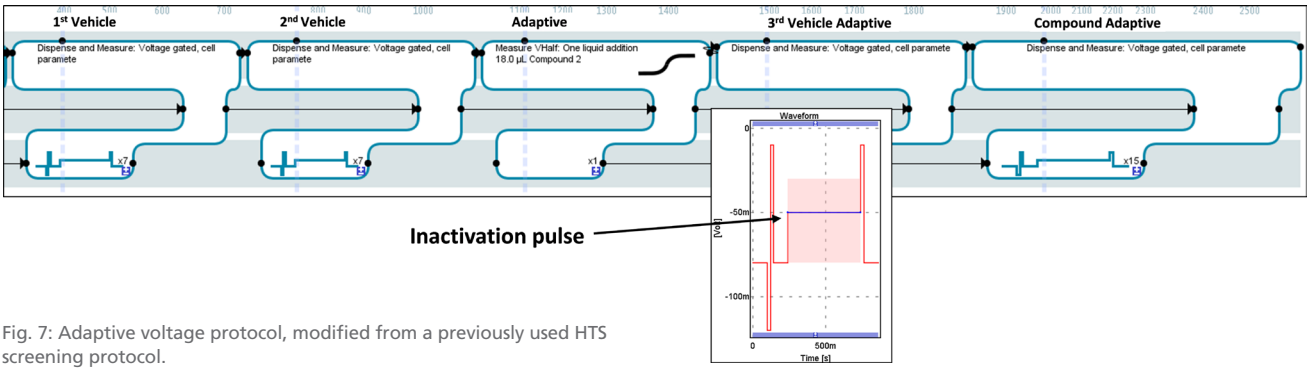

Fig. 7: Adaptive voltage protocol, modified from a previously used HTS screening protocol.

Authors: Juha Kammonen, Charles River Laboratories and Mads P. G. Korsgaard, Sophion Bioscience A/S

References:

Catterall WA, Goldin AL, Waxman SG (2005). International Union of Pharmacology. XLVII. Nomenclature and Structure-Function Relationships of Voltage-Gated Sodium Channels. Pharmacol Rev. 57, 397-409.

Catterall WA, Swanson T (2015). Structural Basis for Pharmacology of Voltage-Gated Sodium and Calcium Channels. Mol Pharmacol. 88, 141-150.

Ahern CA, Payandeh J, Bosmans F, Chanda B (2015). The hitchhiker's guide to the voltage-gated sodium channel galaxy. J Gen Physiol. 147, 1-24.

Bennett DL, Clark AJ, Huang J, Waxman SG, Dib-Hajj SD (2019). The Role of Voltage-Gated Sodium Channels in Pain Signaling. Physiol Rev. 99 1079-1151.

Lenaeus M, El-Din TMG, Ing C, Ramanadane K, Pomès R, Zheng N, Catterall W (2017). Closed and open states of a sodium channel. PNAS 114 (15), E3051-E3060.

Sula A, Booker J, Ng LTC, Naylor CE, DeCaen PG, Wallace BA (2017). The complete structure of an activated open sodium channel. Nature Comms 8.

Ahuja S, Mukund S, Deng L, Khakh K, Chang E, Ho H, Shriver S, Young C, Lin S, Johnson J.P., Wu P, Li J, Coons M, Tam C, Brillantes B, Sampang H, Mortara K, Bowman K, Clark K, Estevez A, Xie Z, Verschoof H, Grimwood M, Dehnhardt C, Andrez J, Focken T, Sutherlin D, Safina B, Starovasnik M, Ortwine D, Franke Y, Cohen C, Hackos D, Koth C, Payandeh J (2015). Structural basis of Nav1.7 inhibition by an isoform-selective small-molecule antagonist. Science 18

Alexandrou AJ, Brown AR, Chapman ML, Estacion M, Turner J, Mis MA, Wilbrey A, Payne E, Gutteridge A, Cox P, Doyle R, Printzenhoff D, Lin Z, Marron BE, West C, Swain NA, Storer RI, Stupple PA, Castle NA, Hounshell JA, Rivara M, Randall A, Dib-Hajj SD, Krafte D, Waxman SG, Patel MK, Butt RP, Stevens EB (2016). Subtype-Selective Small Molecule Inhibitors Reveal a Fundamental Role for Nav1.7 in Nociceptor Electrogenesis, Axonal Conduction and Presynaptic Release. PLoS ONE 11(4): e0152405

Theile JW, Fuller MD, Chapman ML (2016). The Selective Nav1.7 Inhibitor, PF-05089771, Interacts Equivalently with Fast and Slow Inactivated Nav1.7 Channels. Mol Pharmacol. 90, 540-548.

Sophion Bioscience A/S, Baltorpvej 154, 2750 Ballerup, Denmark
Phone: +45 4460 8800, E-mail: info@sophion.com

sophion.com